

Article

Not peer-reviewed version

# Development of the Direct Deuteration Method for Amino Acids and Characterization of Deuterated Tryptophan

[Chie Shibazaki](#)<sup>\*</sup>, Misaki Ueda, [Haruki Sugiyama](#), [Takayuki Oku](#), Motoyasu Adachi, [S. Zoë Fisher](#), [Kazuhiro Akutsu-Suyama](#)<sup>\*</sup>

Posted Date: 25 July 2025

doi: 10.20944/preprints202507.2141.v1

Keywords: amino acid; deuteration; optical isomer; crystal; isotope effect



Preprints.org is a free multidisciplinary platform providing preprint service that is dedicated to making early versions of research outputs permanently available and citable. Preprints posted at Preprints.org appear in Web of Science, Crossref, Google Scholar, Scilit, Europe PMC.

Copyright: This open access article is published under a Creative Commons CC BY 4.0 license, which permit the free download, distribution, and reuse, provided that the author and preprint are cited in any reuse.

*Article*

# Development of the Direct Deuteration Method for Amino Acids and Characterization of Deuterated Tryptophan

Chie Shibazaki <sup>1,\*</sup>, Misaki Ueda <sup>2</sup>, Haruki Sugiyama <sup>3</sup>, Takayuki Oku <sup>1</sup>, Motoyasu Adachi <sup>4</sup>, Zoë Fisher <sup>5,6</sup> and Kazuhiro Akutsu-Suyama <sup>2,\*</sup>

<sup>1</sup> J-PARC Center, Japan Atomic Energy Agency (JAEA), 2-4 Shirakata, Tokai-mura, Naka-gun, Ibaraki 319-1195, Japan

<sup>2</sup> Neutron Science and Technology Center, Comprehensive Research Organization for Science and Society (CROSS), 162-1 Shirakata, Tokai-mura, Naka-gun, Ibaraki 319-1106, Japan

<sup>3</sup> Neutron Industrial Application Promotion Center, Comprehensive Research Organization for Science and Society (CROSS), 162-1 Shirakata, Tokai-mura, Naka-gun, Ibaraki 319-1106, Japan

<sup>4</sup> Institute for Quantum Life Science, National Institutes for Quantum Science and Technology (QST), 4-9-1 Anagawa, Inage, Chiba 263-8555, Japan

<sup>5</sup> European Spallation Source ERIC, P.O. Box 176, SE-221 00 Lund, Sweden

<sup>6</sup> Lund Protein Production Platform, Department of Biology, Lund University, Sölvegatan 35, 22362, Lund, Sweden

\* Correspondence: shibaza@post.j-parc.jp (C.S.), k\_akutsu@cross.or.jp (K.A.)

## Abstract

Proteins and peptides are essential biomolecules involved in the maintenance of biological functions and disease development. Their structural and functional analyses are crucial for drug discovery and pathology. Amino acids, the fundamental building blocks of these biomolecules, are increasingly utilized in deuterated forms in diverse fields, such as metabolic tracing and neutron scattering studies. In this study, we have developed an efficient deuteration method that targets all 20 proteinogenic amino acids, including their side chains. Using a Pt/C-catalyzed hydrogen–deuterium exchange reaction, the reaction parameters were optimized to achieve the selective and stable incorporation of deuterium. In addition, the resulting deuterated compounds, focusing on tryptophan, were characterized in order to assess their physicochemical properties. Because the deuteration reaction caused significant racemization of amino acids, deuterated D/L-tryptophan was isolated using a chiral separation method. Deuterated tryptophan characterization studies confirmed that the photostability was markedly enhanced by deuteration, whereas the acid stability showed no clear isotopic effect. The X-ray crystal structure analyses revealed minimal changes upon the hydrogen-to-deuterium substitution. These results provide a robust platform for the supply of deuterated amino acids, facilitating their application in drug development, structural analysis, and creation of advanced functional biomaterials.

**Keywords:** amino acid; deuteration; optical isomer; crystal; isotope effect

## 1. Introduction

Proteins and polypeptides are fundamental components of biological structures such as muscles, skin, and internal organs, and they play essential roles in maintaining cellular functions. These macromolecules function in diverse physiological processes such as enzymes, hormones, antibodies, and other bioactive agents, contributing to digestion, metabolism, immunity, and intercellular signaling. Malfunctions or structural abnormalities in biomolecules, particularly those involved in

physiological activity, are known to cause various diseases, making them critical targets for biomedical research and drug discovery [1–3].

Amino acids, the building blocks of proteins, form polypeptides through specific sequences of 20 standard types, each contributing to the final three-dimensional structure and function of the protein. In addition to their structural roles, amino acids serve as precursors of neurotransmitters and hormones. For example, glutamic acid functions as an excitatory neurotransmitter and is a known precursor of  $\gamma$ -aminobutyric acid (GABA) and a key intermediate in amino acid metabolism [4]. Similarly, tryptophan is a biosynthetic precursor of serotonin and melatonin compounds involved in the regulation of mood, sleep, and circadian rhythms, making it an important modulator of physiological functions in the central nervous system [5,6].

Metabolic tracing and pharmacokinetic analysis are essential to elucidate how nutrients and bioactive compounds are metabolized in vivo and to clarify how metabolic pathways and intermediates are altered in conditions such as cancer or metabolic disorders. In this context, deuterium-labeled amino acids, in which hydrogen atoms are replaced with deuterium atoms, have proven to be effective tracers [7]. Moreover, the pharmaceutical field has seen growing interest in the use of deuterium isotopes to enhance drug performance [8,9]. Because carbon–deuterium (C–D) bonds are stronger than carbon–hydrogen (C–H) bonds, they confer greater metabolic and photochemical stability, which can improve the pharmacokinetics of drugs that are rapidly degraded in vivo. This has led to increasing interest in the development of deuterated drugs.

The structural and functional analyses of biomolecules often rely on X-ray scattering and diffraction techniques. Recently, neutron scattering has emerged as a powerful complementary method because of its high sensitivity to light elements, particularly deuterium ( $^2\text{H}$ ) [10,11]. By substituting hydrogen atoms in a sample with deuterium, researchers can exploit the differences in neutron scattering cross sections to reduce background noise and enhance contrast in specific regions [12]. Furthermore, site-selective deuteration enables the acquisition of high-resolution information on conformational dynamics and structural changes in targeted domains [13].

In pursuit of these applications, recent studies have demonstrated that ruthenium catalysts are effective for deuterating both the main chain and side chains of specific amino acids [14,15]. In addition, Sajiki et al. developed H–D exchange reactions that introduce deuterium into amine and carboxylic acid compounds by replacing the C–H bonds with C–D bonds using palladium or platinum on carbon catalysts [16,17]. Therefore, it can be suggested that palladium or platinum on carbon-catalyzed deuteration reactions are effective for the deuteration of amino acids. Note that palladium or platinum in carbon-catalyzed deuteration reactions racemizes optical isomers [18] and may racemize amino acids as well.

Despite these aforementioned advancements, the synthesis of deuterated compounds, especially those involving side-chain deuteration, remains expensive and technically challenging. Moreover, reports on the enantioseparation (chiral resolution) and physicochemical characterization of deuterated amino acids are limited.

In this study, we aimed to develop a practical and efficient method for the selective deuteration of 20 proteinogenic amino acids, including their side chains, and to establish a protocol for enantiomeric separation. We evaluated the physicochemical properties of the resulting compounds, including their stability under ultraviolet (UV) irradiation and acidic conditions, to explore their potential use as high-performance biomaterials. Through this study, we aim to contribute to the creation of a sustainable and cost-effective supply platform for deuterated amino acids with applications in drug development, structural biology, and materials science.

Particular attention has been paid to tryptophan, an amino acid of significant interest because of its role as a serotonin and melatonin precursor. Given its relevance in the fields of nutraceuticals and pharmaceuticals, our study focused on the enantioseparation and physicochemical characterization of deuterated tryptophan.

## 2. Materials and Methods

### 2.1. Samples and Reagents

Amino acids (TCI Chemicals Co., Ltd., Japan), activated carbon (Osaka Gas Chemical Co., Ltd.), Platinum on Carbon catalyst (Pt/C) (3 wt% Pt, Type STD (wetted with water), N.E. CHEMCAT Co., Japan), 2-propanol (FUJIFILM Wako Pure Chemical Co., Japan), deuterium oxide (D<sub>2</sub>O) for deuteration and Nuclear Magnetic Resonance (NMR) solvent (99.9% D, Sigma-Aldrich), dimethyl sulfoxide (FUJIFILM Wako Pure Chemical Co., Japan), and methanol (FUJIFILM Wako Pure Chemical Co., Japan) were used without further purification. Ultrapure water (18.2 MΩ.cm) was produced with a deionized purified water production system (RFU424TA system, ADVANTEC, Japan) and used throughout this study.

### 2.2. Configuration of a Simplified Deuteration Apparatus Used for Deuteration

Deuterated amino acid synthesis was performed by sealing the reaction mixture in a small autoclave-type high-pressure reactor (100 mL capacity; Huanyu) equipped with an inner Teflon liner. The reactor was placed in an aluminum bead bath (inner diameter: 130 mm, depth: 160 mm; Tokyo Rikakikai Co., Ltd.) filled with aluminum beads (Tokyo Rikakikai Co., Ltd.) and heated using a hot-plate magnetic stirrer (RCH-1000, Tokyo Rikakikai Co., Ltd.).

### 2.3. Procedure for Deuteration of Amino Acids

A mixture of amino acids (1 g) and Pt/C (3 wt% Pt, 0.40 g, 0.06 mmol) in 2-propanol (4 mL)/D<sub>2</sub>O (40 mL) was loaded into the reactor. The mixture was then heated to 200–70 °C and stirred continuously for one to several days. After cooling to 20 °C, the Pt/C catalyst was then removed by celite filtration and further filtered through a 0.22 μm filter. The filtrate was evaporated to dryness under reduced pressure to obtain deuterated amino acids.

### 2.4. Analytical Methods Using NMR to Determine the Deuteration Level of Amino Acids

The <sup>1</sup>H and <sup>2</sup>H NMR spectra of the deuterated amino acids were recorded using a 400 MHz NMR spectrometer (JEOL JMT-400/54/JJ/YH spectrometer, <sup>1</sup>H: 400 MHz, <sup>2</sup>H: 61.4 MHz) to confirm the deuteration level of the amino acids. Details of the sample preparation method for NMR measurements are provided in the Supporting Information.

### 2.5. Measurement of Optical Rotation

The specific rotation of the samples was measured using a polarimeter (Model P-2200, JASCO, Japan) modified for acid resistance and equipped with a Peltier thermostated cell holder (PTC-262). The measurements were performed at 20 °C using a cylindrical quartz cell (100 mm × 3.5 mm, optical path length: 10 cm) at a wavelength of 598 nm. Each measurement was performed five times and the average value was used. The observed optical rotations were measured under identical conditions, and the specific rotation  $[\alpha]_{D^{20}}$  values were calculated accordingly. All of the measurements were conducted in accordance with standard polarimetric procedures. Commercial L-tryptophan (L-Trp) was dissolved in distilled water at a concentration of 0.9690% (w/v). The solution was heated to 80 °C to ensure complete dissolution before measurement. Deuterated L-tryptophan was dissolved in distilled water at a concentration of 0.56277% (w/v). Complete dissolution was achieved by heating the solution to 90 °C.

### 2.6. Liquid Chromatography Setup for Enantiomeric Separation

High-performance liquid chromatography (HPLC) analysis was conducted using a HITACHI Chromaster system equipped with a Hitachi 5440AD fluorescence detector (excitation at 280 nm and emission at 350 nm). Enantiomeric separation was performed using a DAICEL CHIRALPAK ZWIX(+) column (4.0 mm I.D. × 250 mm L, 3 μm particle size) at a flow rate of 0.15 mL/min. The mobile phase consisted of methanol, acetonitrile, and water at a ratio of 39:39:22 (v/v/v),



supplemented with 40 mM formic acid and 20 mM diethylamine. Commercial L-tryptophan (L-Trp) was dissolved in water by heating at 80 °C to prepare a 20.0 mM stock solution. This solution was diluted 100-fold with the eluent, yielding a final concentration of 0.2 mM. An injection volume of 1  $\mu$ L, corresponding to 2.0 pmol of L-Trp, was used for the HPLC analysis. Deuterated tryptophan (d-Trp) was prepared by dissolving water at 90 °C to obtain a 20.0 mM stock solution. Following 100-fold dilution with the eluent, the final concentration was 0.2 mM. A 1  $\mu$ L aliquot, equivalent to 2.0 pmol of d-Trp, was injected into the HPLC system.

### 2.7. Fluorescence Measurement Method for Evaluating UV-Induced Degradation and Acid-Induced Changes

To measure the UV-induced degradation of tryptophan, samples were irradiated with UV light at 254 nm using a fluorescence spectrophotometer (FP-8300, JASCO Corporation, Japan). The intensity of the UV light was 62.94 mJ/min/cm<sup>2</sup> at the center of the sample. Tryptophan fluorescence measurements were performed using an FP-8300 fluorescence spectrophotometer with an excitation wavelength of 290 nm and an emission range of 295–450 nm. For the analysis of the fluorescence intensity changes under acidic conditions, 6 M hydrochloric acid (FUJIFILM Wako Pure Chemical Co., Japan) was used, and the sample was heated at 80 °C while monitoring the fluorescence intensity at 339 nm.

### 2.8. Crystallization

Deuterated tryptophan (d-Trp), protonated tryptophan (h-Trp), deuterated tryptophan hydrochloride (d-TrpCl), and protonated tryptophan hydrochloride (h-TrpCl) crystals were prepared. A suitable crystal was mounted on a glass capillary and transferred to the rugged two-axis goniometer of a RIGAKU diffractometer with equipped with mirror monochromated Mo-K $\alpha$  radiation ( $\lambda = 0.71073$  Å) and HyPix-6000HEIC detector. The cell parameters were determined and refined, and the raw frame data were integrated using CrysAlisPro 1.171.43.98a (Rigaku OD, 2023). The details of the sample preparation method for X-ray crystallography measurements are described in the Supporting Information.

## 3. Results and Discussion

### 3.1. Deuteration of 20 Proteinogenic Amino Acids

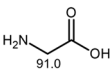
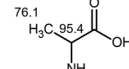
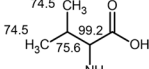
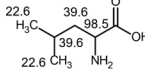
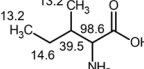
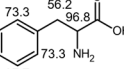
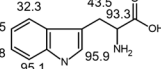
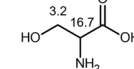
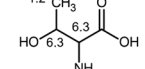
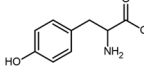
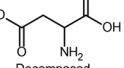
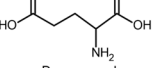
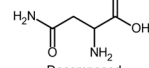
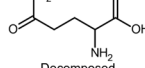
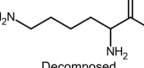
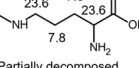
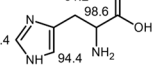
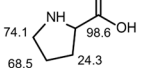
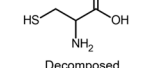
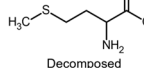
In this study, we developed an efficient deuteration method for 20 proteinogenic amino acids, including side chains, based on the procedure reported by Sawama et al. [19–21]. Commercially available L-amino acids (alanine, arginine, asparagine, aspartic acid, cysteine, glutamine, glutamic acid, glycine, histidine, isoleucine, leucine, lysine, methionine, phenylalanine, proline, serine, threonine, tryptophan, tyrosine, and valine) were used as starting materials. Each amino acid, along with Pt/C catalyst, 2-propanol, and D<sub>2</sub>O, was placed in a Teflon-lined high-pressure vessel for the reaction. The vessel was stirred to ensure temperature uniformity and then heated to conduct the reaction. The degree of deuterium incorporation was evaluated using nuclear magnetic resonance (NMR) spectroscopy.

Initially, deuteration reactions were carried out under standard conditions at 200 °C for 24 h for all 20 amino acids (Fig. S1). Glycine, phenylalanine, and histidine showed average deuteration levels exceeding 80%, with incorporation rates of 91.0%, 80.7%, and 82.5%, respectively. The  $\alpha$ -position (backbone C–H) was almost fully deuterated, with deuteration rates of 91.0%, 96.8%, and 98.6%, respectively, suggesting near-complete deuteration of both backbone and side chain under these conditions (Table S1). Proline also achieved an overall average deuterium incorporation rate of 61.8%, suggesting that increasing the reaction temperature may further enhance the extent of deuteration.

In contrast, amino acids with aliphatic hydrocarbon side chains (alanine, valine, leucine, and isoleucine) and the cyclic hydrocarbon proline exhibited high backbone deuteration (97.0%, 96.5%, 96.5%, 97.5%, and 98.6%, respectively), but their side chains showed poor deuterium incorporation. These results suggest that efficient interaction between the  $\alpha$ -carbon and the catalyst, whereas

interaction with the side-chain carbon atoms appears insufficient. The remaining amino acids decomposed under the same conditions, as confirmed by NMR analysis.

To improve the overall deuteration efficiency, the reaction conditions were optimized by varying the temperature, employing additives, and testing different metal catalysts (Figure 1).

<div style="text-align: center;"> <math>\xrightarrow[\text{(Additives, reaction temperature, reaction time)}]{\text{Pt/C}}</math>            Substrate <math>\longrightarrow</math> Substrate-<math>d_n</math>            2-propanol/<math>D_2O</math> </div>				
 91.0 91.0% (N/A, 200°C) Glycine	 76.1, 95.4 80.9% ( $NH_3$ , 230°C, 152hour) Alanine	 74.5, 74.5, 99.2, 75.6 77.8% ( $CH_3COOH$ , 200°C) Valine	 22.6, 39.6, 98.5, 39.6, 22.6 35.3% ( $CH_3COOH$ , 200°C) Leucine	 13.2, 13.2, 14.6, 98.6, 39.5 16.7% ( $CH_3COOH$ , 200°C) Isoleucine
 97.7, 73.3, 56.2, 96.8, 94.7, 73.3 80.7% (N/A, 200°C) Phenylalanine	 91.5, 32.3, 43.5, 93.3, 89.8, 95.1, 95.9 73.1% ( $NH_3$ , 170°C) Tryptophan	 3.2, 16.7 7.7% (N/A, 100°C) Serine	 1.2, 6.3, 6.3 3.3% (Ru/C, 100°C) Threonine	 Decomposed (N/A, 200°C) Tyrosine
 Decomposed (N/A, 200°C) Aspartic acid	 Decomposed (N/A, 200°C) Glutamic acid	 Decomposed (N/A, 200°C) Asparagine	 Decomposed (N/A, 200°C) Glutamine	 Decomposed (N/A, 100°C) Lysine
 23.6, 7.8, 23.6, 7.8 Partially decomposed 14.6% (N/A, 100°C) Arginine	 97.4, 61.2, 98.6, 94.4 82.5% (N/A, 200°C) Histidine	 74.1, 68.5, 24.3, 98.6 61.8% (N/A, 200°C) Proline	 Decomposed (N/A, 100°C) Cysteine	 Decomposed (N/A, 200°C) Methionine

**Figure 1.** Deuteration results of 20 standard amino acids. Each amino acid (1 g) was reacted in a mixture of 2-propanol (4 mL), Pt/C, and  $D_2O$  within the reaction vessel. The conditions indicated in parentheses refer to any additives (e.g., acetic acid or ammonia), reaction temperature, and reaction time (only shown when exceeding 24 hours). An asterisk indicates that only Ru/C was used as the metal catalyst, with no Pt/C added. The numbers displayed next to each molecular structure represent the deuteration rate; italicized values indicate the mean deuteration level, as determined by NMR spectroscopy.

Alanine showed poor side-chain deuteration at 200°C. Acid/base additives are known to enhance the deuteration reactions [22,23]. Therefore, the addition of acetic acid, sodium hydroxide, and ammonia (equimolar) to the alanine substrate was tested. Among these, ammonia most effectively improved side chain deuteration (Table S2). Further optimization revealed that heating at 230°C for 152 h in the presence of ammonia resulted in high deuteration: 95.4% at the backbone and 76.1% at the side chain, giving an overall average of 80.9%. Conversely, sodium hydroxide and acetic acid suppress side-chain deuteration. These findings therefore suggest that the observed effects of acidic/basic additives are not solely due to pH or solubility, and that ammonia may play a catalytic role.

In contrast to alanine, leucine exhibits a decrease in side chain deuteration upon the addition of ammonia, resulting in a low overall deuteration level (13.2%). The overall deuteration rate increased to 35.3% when acetic acid was used (Table S3). Similar trends were observed for both valine and isoleucine, with acetic acid addition increasing the deuteration from 13.8% to 77.8% for valine, and from 12.0% to 16.7% for isoleucine (Figure 1, Table S1).

Phenylalanine and histidine, bearing aromatic and imidazole rings, respectively, exhibited high deuteration levels under the standard 200°C/24h condition. In contrast, tryptophan, which contains an indole ring, decomposed under the same conditions. When ammonia was added and the reaction was conducted at lower temperatures, the decomposition was suppressed. Optimal deuteration was achieved at 170°C, yielding 93.3% backbone deuteration and 73.1% average incorporation (Table S4).

Whereas, tyrosine, which possesses a phenolic hydroxyl group, decomposed at 200°C but it showed no reactivity at 140°C, indicating the need for further condition optimization.

Serine, with a hydroxyl-containing side chain, decomposed above 170°C and showed limited reactivity at 100°C (average 7.7%) (Table S5). Threonine, another hydroxyl-containing amino acid, underwent oxidation or degradation even at 100°C. Because threonine is not normally decomposed at 100°C, this can be considered as Pt/C accelerating the decomposition. To suppress this degradation, the catalyst was changed from the conventional Pt/C to Ru/C. Under these modified conditions (100 °C for 24 h), decomposition was successfully suppressed. However, the deuteration level remains low, indicating that further optimization of the reaction conditions is necessary.

The acidic amino acids, aspartic acid and glutamic acid, as well as their corresponding amides, asparagine and glutamine, were found to decompose at 200 °C (Table S6). A previous report has suggested that Pd catalysts can effectively deuterate aliphatic compounds [24]. These findings indicate the necessity of exploring alternative metal catalysts.

Basic amino acids, such as lysine and arginine, which possess amino groups in their side chains, undergo decomposition even at 100 °C (Table S7). Amines are generally known to poison metal catalysts, although partial deuteration of arginine has also been observed. Future studies should therefore explore the use of acid additives to suppress decomposition and enhance deuteration efficiency.

Cysteine and methionine, which have sulfur in their side chains, could not be deuterated using our method; the cause of this phenomenon remains unknown. The NMR results indicated that most of the cysteine was present in an unreacted form, but small amounts of cystine and other byproducts were formed by the deuteration reaction. The same reaction was performed without the Pt/C catalyst, and the same by-products were formed when the catalyst was added. Therefore, it is reasonable to assume that the byproducts were generated by heating, and that the Pt/C catalyst did not contribute to them. On the other hand, methionine was also not deuterated and no byproducts were found to be formed (methionine is probably more thermally stable than cysteine).

In addition, the chemical compositions of the used Pt/C catalysts were analyzed using X-ray fluorescence spectrometry (XRF) method (the details of the XRF measurements are described in the Supporting Information). Figure 2 shows the XRF spectra of the Pt/C catalyst before and after the deuteration experiments. The XRF spectrum of the Pt/C used for methionine deuteration had a large sulfur peak, whereas the XRF spectrum of the Pt/C used for cysteine deuteration had a small sulfur peak. These results indicated that methionine strongly coordinated to the Pt/C surface, whereas cysteine hardly coordinated to Pt. It is reasonable to suppose that, because the pKa value of the thiol group in cysteine is approximately 8.3, which is protonated in the reaction mixture, the coordination ability of cysteine to Pt is probably weak.

Although cysteine and methionine have similar molecular structures, there are significant differences in their thermal stabilities and strengths of their interactions with platinum. In conclusion, the deuteration of cysteine and methionine could not be achieved, but on the other hand, this study provided important chemical insights into the deuteration reaction and sulfur-containing amino acids.

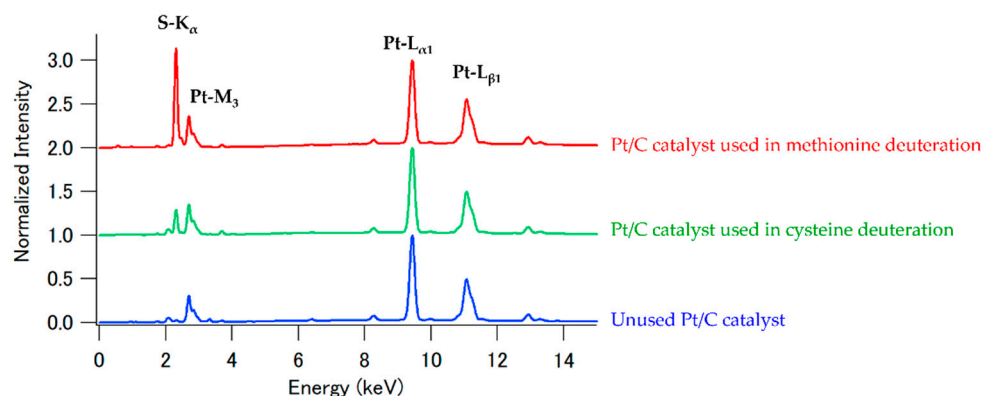


**Figure 2.** The result of the XRF analysis performed on Pt/C samples.

3.2. Chiral Separation of Deuterated Tryptophan

It is well known that small molecules possessing chiral centers may yield stereochemically distinct products when subjected to nucleophilic substitution reactions such as SN2, due to the inversion of the configuration at the reactive center [25]. It is reasonable to suppose that stereo inversion occurs during the substitution of hydrogen atoms directly bonded to the chiral α-carbon of the amino acid backbone with deuterium. In order to investigate whether deuteration alters the optical activity of the amino acids synthesized using the simplified deuteration apparatus, we measured the optical rotation of deuterated L-tryptophan.

As commercially available L-tryptophan is in its naturally occurring non-deuterated form, it is designated as h-L-Trp in this study to clearly distinguish it from deuterated tryptophan (d-Trp). Specifically, we have compared the specific rotation ( $[\alpha]_{D^{20}}$ ) of h-L-Trp with that of d-Trp, which was obtained by deuteration at 170 °C for 24 hours (Table 1). The measured specific rotation of h-L-Trp was consistent with reported literature values (−30.5 to −32.5°), whereas d-Trp exhibited a markedly reduced optical rotation. This significant decrease suggests that the deuteration reaction induced partial epimerization at the chiral α-carbon, resulting in near-racemization of the sample.

**Table 1.** Polarimetric measurement results of tryptophan.

$[\alpha]_{D^{20}}$ (deg·mL·g <sup>−1</sup> ·dm <sup>−1</sup> ) ±SD (20°C、598nm)	Sample
−32.5925 ± 0.0199	L-Tryptophan (h-L-Trp)
−1.6525 ± 0.2656	Deuterated tryptophan (d-Trp)

Based on these findings, we further investigated the enantiomeric composition of deuterated tryptophan using chiral column chromatography to achieve enantiomeric separation.

As an initial step toward obtaining purified d-D-Trp, enantiomeric separation was performed using chiral column chromatography. Figure 3. shows the HPLC profiles of h-L-Trp (top) and tryptophan which we deuterated (bottom). The enantiomers were separated as free amino acids and analyzed using an online fluorescence detection system (350 nm). Because the peak at approximately 36 min was attributed to L-tryptophan, the peaks at approximately 31 and 36 min in the deuterated tryptophan data were attributed to D- and L-tryptophan, respectively. These two peaks were clearly separated, and their respective intensities were nearly identical. Evaluation of the fluorescence peak areas of D- and L-tryptophan suggested that D- and L-tryptophan were present at a ratio of 1:1. The ratio of D- and L-tryptophan was estimated to be 47.5:52.5, based on the obtained optical rotation spectra, and 46.6:53.4, using NMR spectroscopy. Therefore, the fluorescence peak area ratio on the HPLC system is not accurate enough to calculate optical isomer ratio of D- and L-tryptophan.

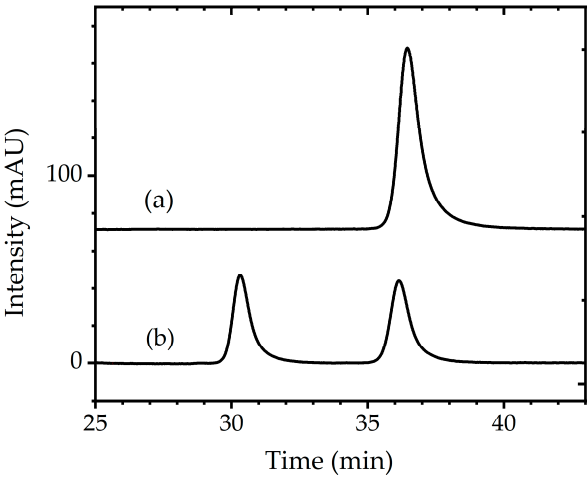




**Figure 3.** Enantiomeric separation using chiral column chromatography. (a) Commercial L-tryptophan (h-L-Trp); (b) Deuterated tryptophan. Detection was performed with excitation at 250 nm and emission at 350 nm.

### 3.3. Physicochemical Characterization of Deuterated Tryptophan

Tryptophan is an amino acid of particular interest in the fields of nutraceuticals and pharmaceuticals because it serves as a biosynthetic precursor for the neurotransmitters serotonin and melatonin [26,27]. However, tryptophan is known to exhibit relatively high photodegradability compared with other amino acids because of the breakdown of its indole ring upon UV absorption [28]. For example, formulations and supplements containing tryptophan may undergo degradation under light or oxidative conditions, potentially reducing their efficacy and generating harmful by-products [29]. Tryptophan degrades slowly in acidic conditions [30,31].

In this study, we have evaluated the effects of deuteration on the acid stability of tryptophan. The progress of degradation was monitored by measuring the changes in fluorescence intensity at 339 nm, the characteristic emission wavelength of tryptophan. Figure 4 and figure S2 show the time-dependent changes in the fluorescence spectrum of tryptophan in 6N HCl aqueous solution at 80°C, and the inset shows the fluorescence intensity changes at 339 nm as a function of reaction time. Because it takes around 60 minutes after preparing the experimental solution at room temperature for the temperature to stabilize at 80°C, the fluorescence spectrum data prior to 60 minutes were excluded from the reaction rate analysis. The fluorescence intensity of tryptophan decreased with increasing reaction time; however, there was no significant difference between the decomposition reactions of protonated and deuterated tryptophan. Although various kinds of decomposition products were generated by the decomposition reaction of tryptophane in 6N HCl solution [32,33], we assumed that the decrease in the fluorescence intensity at 339 nm correlated with tryptophan decomposition. Since chloride anions, which are present in large amounts in the reaction mixture, strongly contribute to the tryptophan decomposition reaction [32], the decomposition rate constant can be calculated according to the following equation (considering it as a pseudo-first-order reaction):

$$\ln C_t = -k_{\text{obs}}t + \ln C_0 \quad (1)$$

where  $k_{\text{obs}}$  is the pseudo-first-order reaction rate constant ( $\text{h}^{-1}$ ) and  $C_t$  and  $C_0$  are the tryptophan concentrations at reaction times  $t = t$  and 0, respectively. The  $k_{\text{obs}}$  values were estimated to be  $0.15 \text{ h}^{-1}$  for h-Trp,  $0.17 \text{ h}^{-1}$  for d<sub>40</sub>-Trp (40% deuterated Trp), and  $0.15 \text{ h}^{-1}$  for d<sub>70</sub>-Trp (70% deuterated Trp), respectively. As mentioned above, since a wide variety of decomposition products must be produced in this reaction, obtained  $k_{\text{obs}}$  values may not be appropriate as reaction rate constants. However, it is clear that there was no significant difference in the  $k_{\text{obs}}$  values. It is reasonable to assume that the concentration of chloride anions in the reaction mixture strongly contributes to the tryptophan decomposition reaction, and the degree of deuteration of tryptophan has no discernible impact on the reaction. That is, isotope effects were negligible in the tryptophan decomposition reaction in the 6N HCl solution.

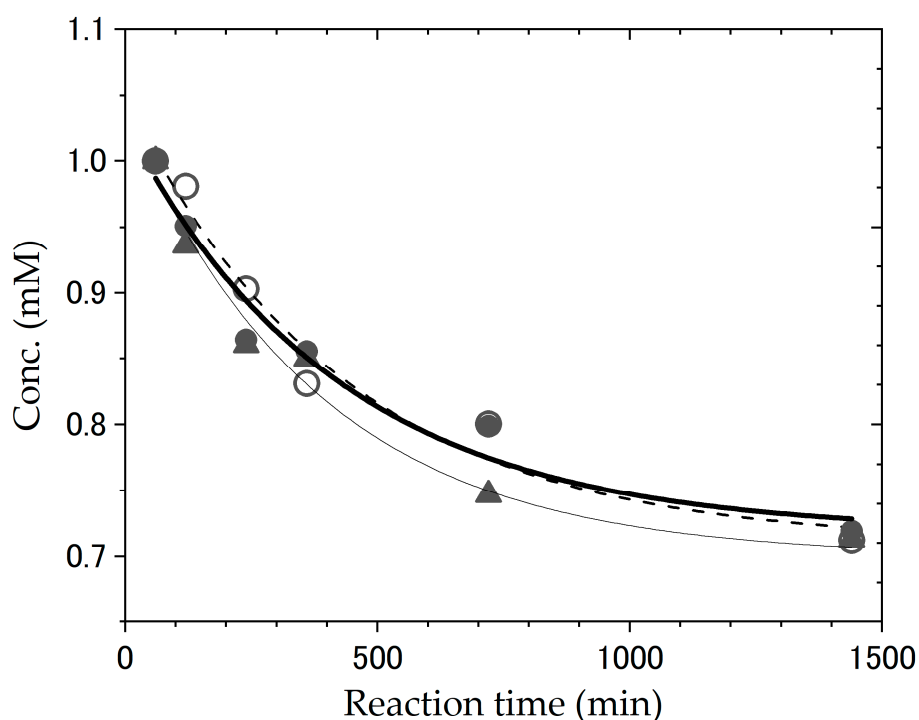


**Figure 4.** Time-dependent fluorescence intensity of tryptophan in acidic aqueous solution. Open circles represent commercially available hydrogenated tryptophan (h-Trp), closed triangles represent 40% deuterated tryptophan (d<sub>40</sub>-Trp), and closed circles represent 70% deuterated tryptophan (d<sub>70</sub>-Trp) synthesized in this study using a simple deuteration apparatus. Dashed, thin, and solid lines indicate the fitted curves for each dataset. The vertical axis indicates tryptophan concentration (mM), and the horizontal axis represents reaction time (min). Fluorescence measurements were performed with an excitation wavelength of 290 nm and an emission wavelength of 339 nm. The sample solutions were prepared at room temperature and required approximately 60 minutes to reach and stabilize at 80 °C; therefore, data collected prior to 60 minutes were excluded from the kinetic analysis.

It is well known that tryptophan is degraded by ultraviolet light through a free radical pathway [28,34], and light shielding is necessary to inhibit its degradation. Deuteration makes tryptophan easier to handle if it is more resistant to UV degradation. In this study, we investigated the effects of isotopes on degradation resistance to ultraviolet light at a wavelength of 254 nm.

Figure 5 and figure S3 show the time-dependent fluorescence change of tryptophan under UV light irradiation in a 100 mM KCl solutions, and the inset shows the fluorescence intensity changes at 354 nm as a function of UV light irradiation time. Although the fluorescence intensities of tryptophan decreased with increasing UV light irradiation time, the fluorescence intensity changes stopped after approximately 20 min of irradiation (0.87 J/cm<sup>2</sup>), after which the fluorescence intensity changed again. Therefore, it is reasonable to assume that the fluorescence intensity of tryptophan changes bi-exponentially.

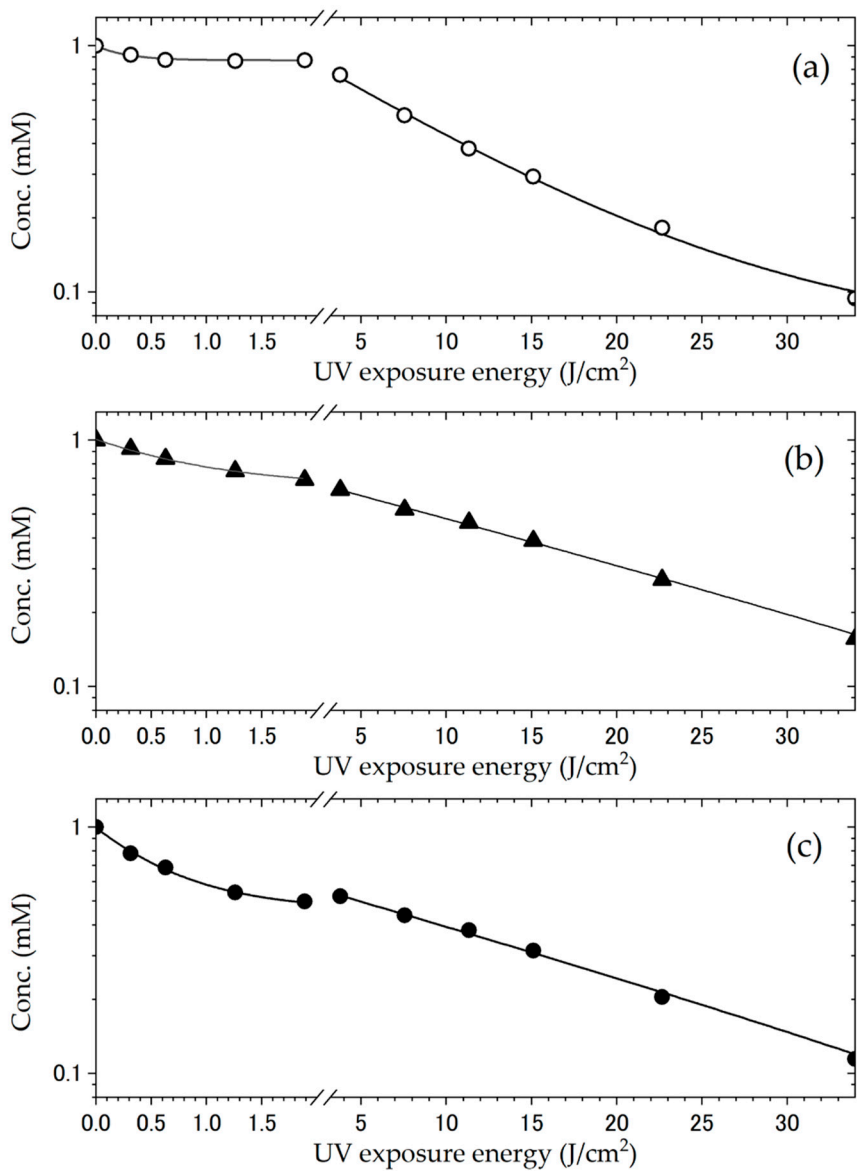


**Figure 5.** Photodegradation of tryptophan under UV irradiation. (a) Commercial tryptophan (h-L-Trp); (b) and (c) 40% and 70% deuterated tryptophan (d<sub>40</sub>-Trp and d<sub>70</sub>-Trp, respectively) synthesized in this study using a simple deuteration apparatus. The graphs show the time-dependent changes in the fluorescence intensity under UV light at 254 nm (62.94 mJ/min/cm<sup>2</sup>) in 100 mM KCl aqueous solution. Fluorescence was measured with an excitation wavelength of 290 nm and an emission range of 295–450 nm.

Previous reports have suggested that the UV degradation of tryptophan is mono-exponential [35,36], but our results are clearly different. Our findings may be attributed to the detailed evaluation of tryptophan UV degradation reactions at irradiation doses of 0–2.0 J/cm<sup>2</sup>. Assuming that the UV degradation of tryptophan is a pseudo-first-order reaction [35], the value of  $k_{\text{obs}}$  can be calculated using Equation (1).

**Table 2.** Summary of the obtained  $k_{\text{obs}}$  and activation energy difference values for the UV degradation reaction.

$k_{\text{obs}}$ (second reaction) and $\Delta E_a$	$k_{\text{obs}}$ (first reaction) and $\Delta E_a$	Sample
0.0061 min <sup>-1</sup>	0.230 min <sup>-1</sup>	h-L-Trp
0.0024 min <sup>-1</sup> , 0.61 kcal/mol	0.065 min <sup>-1</sup> , 0.74 kcal/mol	d <sub>40</sub> -Trp (40% deuterated)
0.0027 min <sup>-1</sup> , 0.48 kcal/mol	0.080 min <sup>-1</sup> , 0.55 kcal/mol	d <sub>70</sub> -Trp (70% deuterated)

The  $k_{\text{obs}}$  values obtained are listed in Table 2. As the degree of tryptophan deuteration increases, the  $k_{\text{obs}}$  value of the UV degradation reaction decreases. Note that the plots of the UV degradation reaction of d<sub>40</sub>-Trp do not appear to be bi-exponential; therefore, it is possible that the calculated  $k_{\text{obs}}$  values of d<sub>40</sub>-Trp are not as reliable as those of the others. In addition, the activation energy ( $E_a$ ) was estimated using the Arrhenius equation given in Equation (2).

$$k_{\text{obs}} = A \exp(-E_a/RT) \quad (2)$$

where  $A$ ,  $R$ , and  $T$  are the pre-exponential factors of the Arrhenius equation, universal gas constant, and temperature, respectively. All UV degradation reactions were performed under the same conditions, with the only major difference being the degree of tryptophan deuteration. Assuming that this pre-exponential factor was the same under these conditions, the difference in  $E_a$  between protonated and deuterated tryptophan was calculated using the Arrhenius equation. According to the calculations, the activation energy difference between these UV degradation reactions was estimated to be approximately 0.48–0.74 kcal/mol. Based on density functional theory (DFT) calculations, the activation energy difference in the hydrogen/deuterium transfer reaction from anisole to methoxy radicals was estimated to be 1–1.5 kcal/mol [37]. The activation energy difference obtained in this experiment is similar to that of the hydrogen/deuterium transfer reaction. Because the dissociation energy of the van der Waals interactions is less than 1 kcal/mol, the stabilizing effect of tryptophan deuteration on the activation energy of the UV degradation reaction was comparable to the van der Waals interaction force. In summary, it can be concluded that deuteration renders tryptophan more resistant to UV light.

### 3.4. Structural Comparison Between Protonated and Deuterated Tryptophan Crystals

Deuterated tryptophan (d-Trp) and its chloride (d-TrpCl) crystallized in this study were racemic mixtures of the D- and L-forms (d-D/L-Trp and d-D/L-TrpCl), as confirmed by single-crystal X-ray diffraction. The crystal structure of d-Trp was dissolved in monoclinic  $P2_1/c$  with one tryptophan molecule to form a racemate ( $Z = 4$ ) (Figure 6, Table S8). D/L-tryptophan adopts a zwitterionic form and forms a dimeric structure through a charge-assisted hydrogen bond ( $N5-H5a \cdots O2$ ) via the crystallographic inversion center. Two additional hydrogen bonds at the amino group ( $N5-H5c \cdots O1$  and  $N5-H5b \cdots O2$ ) link the tryptophan dimer along the  $b$ - and  $c$ -axes, respectively. Its crystal structure is similar to that of nondeuterated tryptophan (h-Trp) [38–40]. The differences in the bond lengths and angles of non-hydrogen atoms between d-Trp and h-Trp amount with maximum deviations of up to 0.01 Å and 0.86°, respectively. (Table S9, S10). The measured values showed a small variation, but this difference was within the standard deviation ( $3\sigma$  range of the experimental error). Similarly, no significant differences were observed between the hydrogen bond lengths of d-Trp and h-Trp (Table S11). Deuterated tryptophan chloride (d-TrpCl) crystallized from a racemic mixture as a racemic conglomerate. The crystal structure was determined to be monoclinic  $P2_1$  with one tryptophan cation and one chloride anion in the asymmetric unit. One chloride anion and three tryptophan cations are linked by hydrogen bonds ( $O1-D1 \cdots Cl16a$ ,  $N1-D5A \cdots Cl16$ ,  $N1-D5B \cdots Cl16$ ,  $N1-D5C \cdots Cl16$ ), resulting in three-dimensional hydrogen bond networks (Figure 7, Table S8). The crystal structure was similar to that of non-deuterated tryptophan chloride crystals (h-TrpCl) [41]. There were no significant differences in the bond lengths, angles, and hydrogen bond lengths between d-TrpCl and h-TrpCl; the maximum deviations of 0.002 Å (bond lengths) and 0.26° (bond angles) (Table S12, S13, and S14). For the crystal structure refinement, the deuterium (or hydrogen atom) positions and thermal parameters were refined without any structural restraints. The differences in the C-D, N-D, and O-D bond lengths between d-TrpCl and h-TrpCl were within the standard deviation. In this study, hydrogen–deuterium exchange did not affect the bond lengths, angles, or intermolecular interactions in the crystal structures of tryptophan.

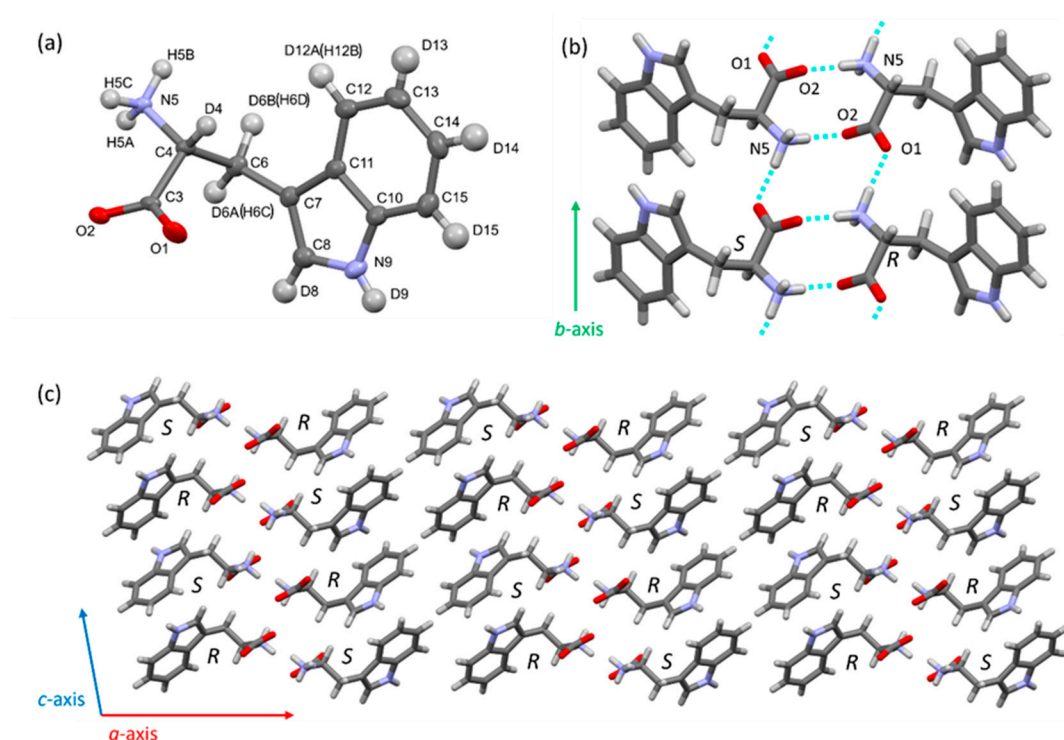


**Figure 6.** (a) Crystal structures of the deuterated tryptophan (d-Trp) as ellipsoid model with a probability of 50%. (b) Hydrogen bond (N5–H5a ... O2) between (S)-tryptophan and (R)-tryptophan molecules forms a dimer structure. Another hydrogen bond (N5–H5c ... O1) linked the tryptophan dimers along the b-axis. (c) Crystal packing of tryptophan.

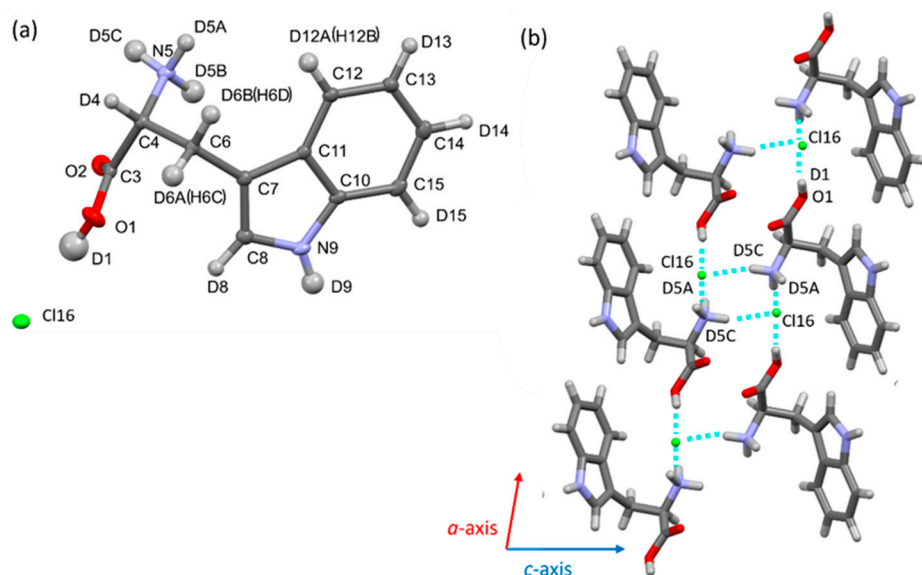


**Figure 7.** (a) Crystal structure of the deuterated tryptophan chloride (d-TrpCl) as ellipsoid model with a probability of 50%. The crystals were obtained as racemic conglomerate, the structure analyzed crystal consists of (R)-tryptophan. (b) Tryptophane cations and chloride anions are linked to form three-dimensional hydrogen bond network.

#### 4. Conclusions

In this study, we aimed to establish an efficient deuteriation method for 20 proteinogenic amino acids, including their side chains, based on a platinum-on-carbon (Pt/C)-catalyzed hydrogen–deuterium exchange reaction. By optimizing the key reaction parameters, such as temperature,



reaction time, additives, and metal catalysts, we significantly improved both the selectivity and stability of the process.

Nine amino acids achieved main-chain deuteration levels exceeding 90%, and six amino acids exhibited average deuteration levels above 70% when side chains were also included. Notably, valine, phenylalanine, and histidine—amino acids, whose deuterated forms remain costly in the commercial market as of 2025, were efficiently and reproducibly synthesized using this method, highlighting its practical utility. In addition, decomposition-prone amino acids, such as serine and threonine, were successfully stabilized by careful temperature control and catalyst selection.

A particularly striking finding was the significant decrease in optical rotation observed for deuterated amino acids, indicating substantial racemization during the reaction. This underscores the need for enantiomeric separation to preserve the optical purity. Indeed, the chiral separation of tryptophan using a chiral column enabled the successful synthesis and isolation of deuterated D-tryptophan, a compound that is not commercially available.

Evaluation of the physicochemical properties revealed that while no clear isotope effect was observed for acid stability (tested in 6N HCl), a marked improvement in photostability was achieved. This suggests that deuteration is a promising strategy to enhance the photostability of amino acids.

Single-crystal X-ray diffraction analysis of deuterated tryptophan showed no significant changes in the bond lengths, bond angles, or intermolecular interactions upon hydrogen–deuterium substitution.

Collectively, these findings have established a practical and versatile platform for the stable supply of deuterated amino acids and peptides. This method has strong potential for application not only in neutron-based structural analysis and pharmacokinetic studies, but also in the development of next-generation pharmaceuticals, functional foods, and biomaterials.

**Supplementary Materials:** The following supporting information can be downloaded at the website of this paper posted on Preprints.org. Additional data are available in the Supplementary Information.

**Author Contributions:** Conceptualization, K.A. and C.S.; methodology, K.A. and C.S.; software, K.A., C.S. and H.S.; validation, K.A., C.S. and H.S.; formal analysis, K.A., C.S. and H.S.; investigation, K.A., C.S. and H.S.; resources, C.S.; data curation, K.A., C.S. and H.S.; writing—review and editing, K.A. and C.S.; supervision, M.A. and Z.F.; project administration, T.O. All authors have read and agreed to the published version of the manuscript.

**Funding:** This research was supported by the Japan Society for the Promotion of Science (JSPS) KAKENHI Grant-in-Aid for Scientific Research (C) (21K05121) and the JAEA Seed Research and Development Program (HOUGA).

**Institutional Review Board Statement:** Not applicable.

**Informed Consent Statement:** Not applicable.

**Data Availability Statement:** The original contributions presented in this study are included in the article. Further inquiries can be directed to the corresponding authors.

**Acknowledgments:** Chemical deuteration experiments and NMR analyses were conducted at the CROSS User Experiment Preparation Room III and J-PARC MLF Deuteration Laboratory, respectively. The SAKURA mobility grant was awarded to SZF to visit to J-PARC and was funded by Vetenskapsrådet (VR) in the Intsam initiative, administered and awarded by European Spallation Source (ESS) and the JAEA Seed Research and Development Program (HOUGA). We would like to thank Editage (www.editage.jp) for English language editing.

**Conflicts of Interest:** The authors declare no conflicts of interest.

## Abbreviations

The following abbreviations are used in this manuscript:

L-Trp	The optically active L-form of tryptophan
D-Trp	The optically active D-form of tryptophan
h-Trp	Protiated tryptophan
d-Trp	Deuterated tryptophan
d-L-Trp	Deuterated L-form of tryptophan
d-D-Trp	Deuterated D-form of tryptophan

## References

1. Wang, L.; Wang, N.; Zhang, W.; Cheng, X.; Yan, Z.; Shao, G.; Wang, X.; Wang, R.; Fu, C. Therapeutic peptides: current applications and future directions. *Signal Transduct. Target. Ther.* 2022, 7, 48.
2. Ito, K.; Matsuda, Y.; Mine, A.; Shikida, N.; Takahashi, K.; Miyairi, K.; Shimbo, K.; Kikuchi, Y.; Konishi, A. Single-chain tandem macrocyclic peptides as a scaffold for growth factor and cytokine mimetics. *Commun. Biol.* 2022, 5, 56.
3. Hopkins, A.L.; Groom, C.R. The druggable genome. *Nat. Rev. Drug Discov.* 2002, 1, 727–730.
4. Schousboe, A.; Bak, L.K.; Waagepetersen, H.S. Astrocytic control of biosynthesis and turnover of the neurotransmitters glutamate and GABA. *Front. Endocrinol.* 2013, 4, 102.
5. Höglund, E.; Øverli, Ø.; Winberg, S. Tryptophan metabolic pathways and brain serotonergic activity: a comparative review. *Front. Endocrinol.* 2019, 10, 158.
6. Richard, D.M.; Dawes, M.A.; Wurtman, C.; et al. L-tryptophan: basic metabolic functions, behavioral research and therapeutic indications. *Int. J. Tryptophan Res.* 2009, 2, 45–60.
7. Kim, T.-Y.; Wang, D.; Kim, A.K.; Lau, E.; Lin, A.J.; Liem, D.A.; Zhang, J.; Zong, N.C.; Lam, M.P.Y.; Ping, P. Metabolic labeling reveals proteome dynamics of mouse mitochondria. *Mol. Cell. Proteomics* 2012, 11, 1586–1594.
8. Harbeson, S.L.; Tung, R.D. Deuterium medicinal chemistry: a new approach to drug discovery and development. *MedChem News* 2014, 24(2), 8–22.
9. Russak, E.M.; Bednarczyk, E.M. Impact of deuterium substitution on the pharmacokinetics of pharmaceuticals. *Ann. Pharmacother.* 2019, 53(2), 211–216.
10. Oksanen, E.; Chen, J.C.-H.; Fisher, S.Z. Neutron crystallography for the study of hydrogen bonds in macromolecules. *Molecules* 2017, 22(4), 596.
11. Shibasaki, C.; Shimizu, R.; Kagotani, Y.; Ostermann, A.; Schrader, T.E.; Adachi, M. Direct observation of the protonation states in the mutant green fluorescent protein. *J. Phys. Chem. Lett.* 2020, 11, 492–496.
12. Krueger, S. Small-angle neutron scattering contrast variation studies of biological complexes: Challenges and triumphs. *Curr. Opin. Struct. Biol.* 2022, 74, 102375.
13. Bradshaw, J.P. Orientation of the headgroup of phosphatidylinositol in a model biomembrane as determined by neutron diffraction. *Biochemistry* 1999, 38, 8393–8401.
14. Chatterjee, B.; Krishnakumar, V.; Gunanathan, C. Selective  $\alpha$ -Deuteration of Amines and Amino Acids Using D<sub>2</sub>O. *Org. Lett.* 2016, 18, 5892–5895.
15. [15\_ CST24Mencia] Mencia, G.; Rouan, P.; Fazzini, P.F.; Kulyk, H. Catalytic enantiospecific deuteration of complex amino acid mixtures with ruthenium nanoparticles. *Catal. Sci. Technol.* 2024, 14, 4904–4911.
16. Sawama, Y.; Matsuda, T.; Moriyama, S.; Ban, K.; Fujioka, H.; Kamiya, M.; Shou, J.; Ozeki, Y.; Akai, S.; Sajiki, H. Unprecedented regioselective deuterium-incorporation of alkyltrimethylammonium chlorides and Raman analysis. *Asian J. Org. Chem.* 2023, e202200710.
17. Sawama, Y.; Park, K.; Yamada, T.; Sajiki, H. New gateways to the platinum group metal-catalyzed direct deuterium-labeling method utilizing hydrogen as a catalyst activator. *Chem. Pharm. Bull.* 2018, 66, 21–28.
18. Esaki, H.; Ohtaki, R.; Maegawa, T.; Monguchi, Y.; Sajiki, H. Novel Pd/C-catalyzed redox reactions between aliphatic secondary alcohols and ketones under hydrogenation conditions: application to H–D exchange reaction and the mechanistic study. *J. Org. Chem.* 2007, 72, 2143–2150.
19. Sawama, Y.; Park, K.; Yamada, T.; Sajiki, H. New gateways to the platinum group metal-catalyzed direct deuterium-labeling method utilizing hydrogen as a catalyst activator. *Chem. Pharm. Bull.* 2018, 66, 21–28.
20. Akutsu-Suyama, K.; Ueda, M.; Shibasaki, C.; Fisher, Z. Development of a Simple and Easy Chemical Deuteration System. *CROSS Rep.* 2024, 2024, 001.

21. Shibazaki, C.; Suzuki, H.; Ikegami, T.; Yoshida, K.; Oku, T.; Adachi, M.; Akutsu-Suyama, K. Recycling of Used Heavy Water and Its Application to Amino Acid Deuteration. *JSP Conf. Proc.* 2024, submitting.
22. Munz, D.; Webster-Gardiner, M.; Fu, R.; Strassner, T.; Goddard, W. A., III; Gunnoe, T. B. Proton or metal? The H/D exchange of arenes in acidic solvents. *ACS Catal.* 2015, 5, 769–775.
23. Patel, M.; Saunthwal, R. K.; Verma, A. K. Base-mediated deuteration of organic molecules: a mechanistic insight. *ACS Omega* 2018, 3, 10612–10623.
24. [24\_Chem08Kurita] Kurita, T.; Aoki, F.; Mizumoto, T.; Maejima, T.; Esaki, H.; Maegawa, T.; Monguchi, Y.; Sajiki, H. Facile and convenient method of deuterium gas generation using a Pd/C-catalyzed H<sub>2</sub>-D<sub>2</sub> exchange reaction and its application to synthesis of deuterium-labeled compounds. *Chem. Eur. J.* 2008, 14, 3371–3379.
25. [25\_Nature24Lovinger] Lovinger, G.J.; Sak, M.H.; Jacobsen, E.N. Catalysis of an S<sub>N</sub>2 pathway by geometric preorganization. *Nature* **2024**, 632, 1052.
26. Hartmann, E. Effects of L-tryptophan on sleepiness and on sleep. *J. Psychiatr. Res.* 1982, 17, 107–113.
27. Young, S. N. How to increase serotonin in the human brain without drugs. *J. Psychiatr. Neurosci.* 2007, 32, 394–399.
28. Bellmaine, S.; Schnellbaecher, A.; Zimmer, A. Reactivity and degradation products of tryptophan in solution and proteins. *Free Radic. Biol. Med.* 2020, 160, 696–718.
29. Igarashi, N.; Onoue, S.; Tsuda, Y. Photoreactivity of Amino Acids: Tryptophan-Induced Photochemical Events via Reactive Oxygen Species Generation. *Anal. Sci.* 2007, 23, 829–833.
30. Friedman, M.; Finley, J. W. Methods of tryptophan analysis. *J. Agric. Food Chem.* 1971, 19, 626–631.
31. Friedman, M.; Cuq, J.-L. Chemistry, analysis, nutritional value, and toxicology of tryptophan in food. A review. *J. Agric. Food Chem.* **1988**, 36, 1139–1147.
32. Ohta, T. The Decomposition of Tryptophan in Acid Solutions: Specific Effect of Hydrochloric Acid. *Chem. Pharm. Bull.* 1981, 29, 1767–1771.
33. Gotoh, Y.; Shibata, T. Heat Decomposition of Amino Acids with Autoclave (Part 1). *Jpn. J. Home Econ.* 1970, 21, 428–431.
34. Schöneich, C. Novel Chemical Degradation Pathways of Proteins Mediated by Tryptophan Oxidation: Tryptophan Side Chain Fragmentation. *J. Pharm. Pharmacol.* 2018, 70 (5), 655–665.
35. Zhang, K.; Fei, W.; Ji, J.; Yang, Y. Degradation of Tryptophan by UV Irradiation: Influencing Parameters and Mechanisms. *Water* 2021, 13, 2368.
36. Fujii, N.; Uchida, H.; Saito, T. The Damaging Effect of UV-C Irradiation on Lens  $\alpha$ -Crystallin. *Mol. Vis.* 2004, 10, 814–820.
37. Kimura, Y.; Kanematsu, Y.; Sakagami, H.; Rivera Rocabado, D. S.; Shimazaki, T.; Tachikawa, M.; Ishimoto, T. Hydrogen/Deuterium Transfer from Anisole to Methoxy Radicals: A Theoretical Study of a Deuterium-Labeled Drug Model. *J. Phys. Chem. A* **2022**, 126, 155–164.
38. Bera, S.; Xue, B.; Rehak, P.; Jacoby, G.; Ji, W.; Shimon, L. J. W.; Beck, R.; Král, P.; Cao, Y.; Gazit, E. Self-Assembly of Aromatic Amino Acid Enantiomers into Supramolecular Materials of High Rigidity. *ACS Nano* 2020, 14, 1694–1706.
39. Hübschle, C. B.; Messerschmidt, M.; Luger, P. Crystal Structure of DL-Tryptophan at 173 K. *Cryst. Res. Technol.* 2004, 39, 274–278.
40. Li, Y.; Zhao, Y.; Zhang, Y. Solid Tryptophan as a Pseudoracemate: Physicochemical and Crystallographic Characterization. *Chirality* 2015, 27, 88–94.
41. Takigawa, T.; Ashida, T.; Sasada, Y.; Kakudo, M. The Crystal Structures of L-Tryptophan Hydrochloride and Hydrobromide. *Bull. Chem. Soc. Jpn.* 1966, 39, 2369–2378.

**Disclaimer/Publisher's Note:** The statements, opinions and data contained in all publications are solely those of the individual author(s) and contributor(s) and not of MDPI and/or the editor(s). MDPI and/or the editor(s) disclaim responsibility for any injury to people or property resulting from any ideas, methods, instructions or products referred to in the content.

